How to Cite:
Yusufkhan, P. S., Deshmukh, S. R., & Farooqui, M. (2022). Design, synthesis, and biological evaluation of some methyl 2-(1H-pyrazol-4-ylthio)-1,2,3,4-tetrahydro-6-methylpyrimidine-5-carboxylate derivatives as potential DHFR inhibitors. *International Journal of Health Sciences*, *6*(S1), 1018-1040. https://doi.org/10.53730/ijhs.v6nS1.4853

Design, Synthesis, and Biological Evaluation of Some Methyl 2-(1h-Pyrazol-4-Ylthio)-1, 2, 3, 4-Tetrahydro-6-Methylpyrimidine-5-Carboxylate Derivatives as Potential DHFR Inhibitors

Pathan Sherkhan Yusufkhan
Department of Chemistry, Dr. Rafiq Zakaria College for Women, Aurangabad, Maharashtra 431001, India | Department of Chemistry, Kohinoor Arts, Commerce and Science College Khultabad, Aurangabad, Maharashtra 431001, India

Suparna R. Deshmukh
Department of Chemistry, S. K. Gandhi College, Kada, Tal: Ashti, Dist: Beed, Maharashtra 414202, India

Mazahar Farooqui
Department of Chemistry, Maulana Azad College of Arts, Science and Commerce, Aurangabad 431004, India

***Abstract*---**Drug-resistant bacteria pose an increasingly serious threat to mankind all over the world. However, the currently available clinical treatments do not meet the urgent demand. Therefore, it is desirable to find new targets and inhibitors to overcome the problems of antibiotic resistance. Dihydrofolate reductase (DHFR) is an important enzyme required to maintain bacterial growth, and hence inhibitors of DHFR have been proven as effective agents for treating bacterial infections. In the present work, we have designed some methyl 2-(1H-pyrazol-4-ylthio)-1,2,3,4-tetrahydro-6-methylpyrimidine-5-carboxylate derivatives as potential DHFR inhibitors through rational drug design approach. The designed derivatives were screened through Lipinski rule, Veber's rule, ADMET analysis, drug-likeness properties, and molecular docking. All the compounds demonstrated more potent activity than Ampicillin against both gram-positive and gram-negative bacteria. Most of the compounds were more or equipotent than Chloramphenicol and Ciprofloxacin. Compound A7 was sensitive at 25 µg/mL against Escherichia coli, Pseudomonas aeruginosa, and Staphylococcus aureus whereas compound A20 was sensitive to all

International Journal of Health Sciences ISSN 2550-6978 E-ISSN 2550-696X © 2022.
***Corresponding author**: Yusufkhan, P. S.; Email: sherkhanpathan01.91@gmail.com*
Manuscript submitted: 27 Nov 2021, Manuscript revised: 18 Feb 2022, Accepted for publication: 09 March 2022

gram +ve and –ve bacteria at same concentration. Compound A16 was sensitive at 50 µg/mL against all the bacteria. In antifungal activity, compound A7 exhibited MFCs of 100 µg/mL against Candida albicans, Aspergillus niger, and Aspergillus clavatus which is same as Nystatin.

***Keywords*---**antibacterial, biginelli reaction, DHFR, molecular docking, pyrimidines.

Introduction

One of the most serious risks to public health today is the emergence of germs that are resistant to the majority of the common treatment medications(Murali et al., 2014; Sánchez-Sánchez et al., 2017). Drug-resistant bacteria, such as methicillin-resistant Staphylococcus aureus (MRSA) and multidrug-resistant Escherichia coli, cause great difficulties in the treatment of nosocomial infections, which severely threaten global public health(Anwar et al., 2020; Jouhar et al., 2020; Loi et al., 2019). According to a UK Government analysis, "the cost in terms of lost global productivity between now and 2050 will be an astonishing 100 trillion USD if we do not take action". Fungal infections can represent a major hazard to human health, particularly in immunocompromised people. Invasive fungal infections (IFIs) provide a huge worldwide problem in terms of clinical management(Indora and Kaushik, 2015; Marchese et al., 2016; Rahman et al., 2009). As a result, the need for novel antimicrobial agents that are distinct from current agents is emphasized.

The dihydrofolate reductase (DHFR) enzyme has been shown to be a therapeutic target for treating infections since the mid-20th century. In both prokaryotic and eukaryotic cells, DHFR is involved in the creation of raw material for cell proliferation by catalyzing the reduction of dihydrofolate to tetrahydrofolate utilizing NADPH. DHFR inhibitors are frequently used to treat fungal, bacterial, and mycobacterial diseases, as well as to combat malaria. Various compounds and medications have been developed and introduced to the market throughout the years(He et al., 2020; Songsungthong et al., 2021; Wróbel et al., 2020).

Compounds based on the pyrimidine scaffold are known to exhibit many different biological actions such as antibacterial, antifungal, anti-inflammatory and antitumor activities(Mittersteiner et al., 2021; Nerkar, 2021; Verma et al., 2020). Lots of amino pyrimidine-based derivatives have been reported to exhibit antibacterial activities via inhibiting DHFR(Ahmed Elkanzi, 2020; Bhat et al., 2017). Therefore, in present study we have selected pyrimidine scaffold to design and develop some DHFR inhibitors as potential antibacterial and antifungal agents. The designed derivatives were first screened through ADMET property calculations and then those possess drug-likeness properties were subjected for molecular docking studies. The derivatives which found significant DHFR inhibition potential were subjected for wet lab synthesis followed by spectral analysis and biological evaluation.

Materials and Method

Designing of derivatives

In the present work, we have designed some methyl 2-(1*H*-pyrazol-4-ylthio)-1,2,3,4-tetrahydro-6-methylpyrimidine-5-carboxylate derivatives as illustrated in Table 1. After designing of derivatives, all the molecules were subjected for in silico screening to check drug-likeness properties.

Table 1
The designing approach of methyl 2-(1H-pyrazol-4-ylthio)-1,2,3,4-tetrahydro-6-methylpyrimidine-5-carboxylate derivatives

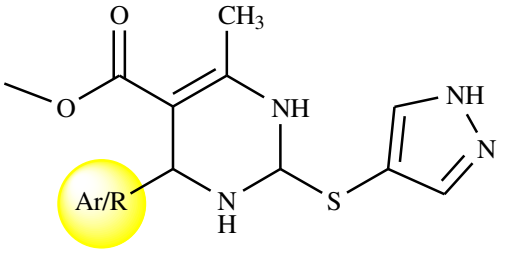

methyl 2-(1*H*-pyrazol-4-ylthio)-1,2,3,4-tetrahydro-6-methylpyrimidine-5-carboxylate derivatives

Compound code	Ar/R	Compound code	Ar/R
A1	—H	A11	—3-hydroxy phenyl
A2	—phenyl	A12	—2,3,4-trihydroxy phenyl
A3	—4-nitro phenyl	A13	—3-methoxy-4-hydroxy phenyl
A4	—4-bromo phenyl	A14	—2-methoxy phenyl
A5	—4-fluoro phenyl	A15	—4-styryl
A6	—4-chloro phenyl	A16	—napthyl
A7	—4-methyl phenyl	A17	—2,4-dinitro phenyl
A8	—4-methoxy phenyl	A18	—4-methylsulfonyl phenyl
A9	—4-hydroxy phenyl	A19	—4-dimethylamino phenyl
A10	—3-nitro phenyl	A20	—4-trifluoromethyl phenyl

Pharmacokinetics and toxicity predictions of designed derivatives

Utilizing molinspiration and SwissADME servers, Lipinski rule of five and pharmacokinetic features of developed derivatives were investigated (Kim et al., 2021; Daina et al., 2017). An in silico toxicity prediction of designed derivatives has been made using ProTox-II, a webserver that is freely available(http://tox.charite.de/protox_II)(Banerjee et al., 2018).

Molecular docking

After screening through in silico ADMET analysis, the screened molecules were subjected for the molecular docking studies. The proposed derivatives and the native ligand were docked against the crystal structure of the wild-type E. coli

dihydrofolate reductase using Autodock vina 1.1.2 in PyRx 0.8 (Dallakyan & Olson, 2015). ChemDraw Ultra 8.0 was used to draw the structures of the intended derivatives and native ligand (mole. File format). All the ligands were subjected for energy minimization by applying Universal Force Field (UFF)(Rappé et al., 1992). RCSB Protein Data Bank (PDB) entry 5CCC contains the wild-type E. coli dihydrofolate reductase complexed with 5,10-dideazatetrahydrofolate and oxidized nicotinamide adenine dinucleotide phosphate (https://www.rcsb.org/structure/5CCC). Discovery Studio Visualizer (version-19.1.0.18287) was used to refine the enzyme structure, purify it, and get it ready for docking(San Diego: Accelrys Software Inc., 2012). A three-dimensional grid box (size_x=39.7765672935Å; size_y=40.0725575009Å; size_z=35.1695000152Å) with an exhaustiveness value of 8 was created for molecular docking (Dallakyan & Olson, 2015). BIOVIA Discovery Studio Visualizer was used to locate the protein's active amino acid residues. The approach outlined by Khan et al. was used to perform the entire molecular docking procedure, identify cavity and active amino acid residues(Chaudhari et al., 2020; S. L. Khan et al., 2021; S.L. Khan et al., 2020; Sharuk L. Khan et al., 2020; Siddiqui et al., 2021). Fig. 1 shows the revealed cavity of DHFR with the co-crystallize ligand molecule.

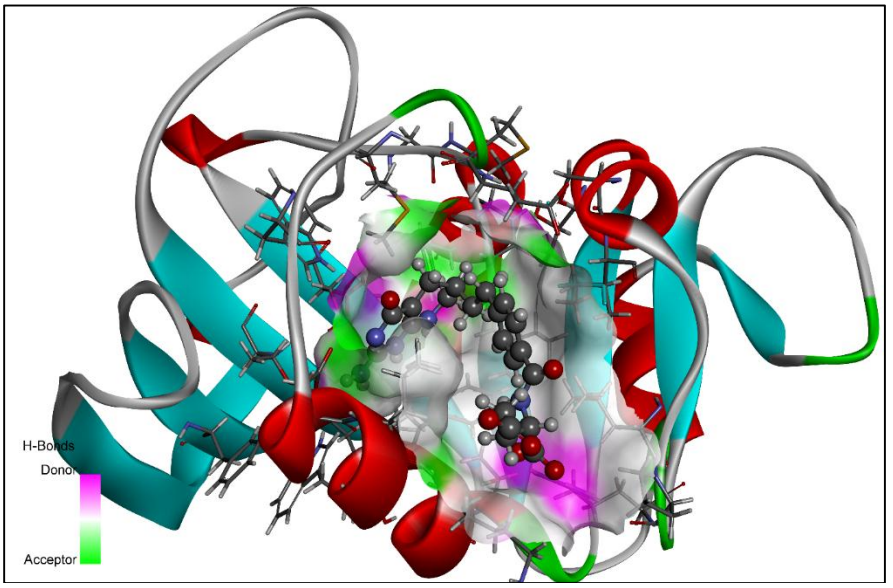

Figure. 1. 3D ribbon view of DHFR with native ligand in allosteric site

Reaction scheme and synthesis of selected derivatives

From in silico screening and molecular docking studies, compounds A7, A16, and A20 were selected for the synthesis. All the required chemicals i.e. ethyl acetoacetate, aldehyde, thiourea, ferric chloride (FeCl3.6H2O), conc. HCl, ethanol, 4-chloropyrazole, potassium hydroxide (KOH), and acetone of synthetic grade were purchased and procured from Lab Trading Laboratory, Aurangabad, Maharashtra, India. The progress of the reaction was confirmed by Thin-layer

chromatography [TLC, (Merck precoated silica GF 254)] and compounds were subjected for spectral analysis by 1H, 13C NMR (on a Varian-VXR-300S at 400 MHz NMR spectrometer) and Mass spectroscopy with chloroform (d6) as the solvent and TMS as the internal standard; chemical shift values were expressed in δ ppm. The melting points were measured using the VEEGO MODEL VMP-D melting point apparatus. The detailed procedure for the synthesis of derivatives is discussed in the below section.

- Step-I: Synthesis of 1,2,3,4-tetrahydropyrimidine-2-thiol
  The reaction is a modified Biginelli reaction that generates 1,2,3,4-tetrahydropyrimidine-2-thiol from ethyl acetoacetate, aldehyde and thiourea[3,4]. A solution of ethyl acetoacetate (1.3gm, 10 mmol), thiourea (1.14gm, 15 mmol), ferric chloride (FeCl3.6H2O, 2.5 mmol) and conc. HCl (1-2 drops) in EtOH (20 mL) was heated independently with appropriate aldehydes (10 mmol), under reflux for 4-5 hrs[5]. After cooling, the reaction mixtures were poured onto crushed ice (100gm). Stirring was continued for several minutes, the solid products were filtered, independently washed with cold H2O (2 times 50 mL) and a mixture of EtOH-H2O, 1:1 (3 times 20 mL). The solids were dried and recrystallized from hot EtOH to afford pure products. The m.p. were recorded and are uncorrected. The yields obtained were in the range of 75-95%.
- Step-II: Synthesis of final pyrimidine derivatives
  4-chloropyrazole (1.66 gm, 0.01 mol.) and 1,2,3,4-tetrahydropyrimidine-2-thiols (0.01 mol.) were condensed by heating with Potassium hydroxide (KOH) and H2O: acetone (2:1) at about 50-60oC for 45 min. Then the reaction mixture cooled to room temperature and then poured into ice-cold water, the precipitate was separated by filtration and recrystallized from ethanol. The yield was 90-95%. The proposed reaction schemes of step-I and step-II are illustrated in Fig. 2.

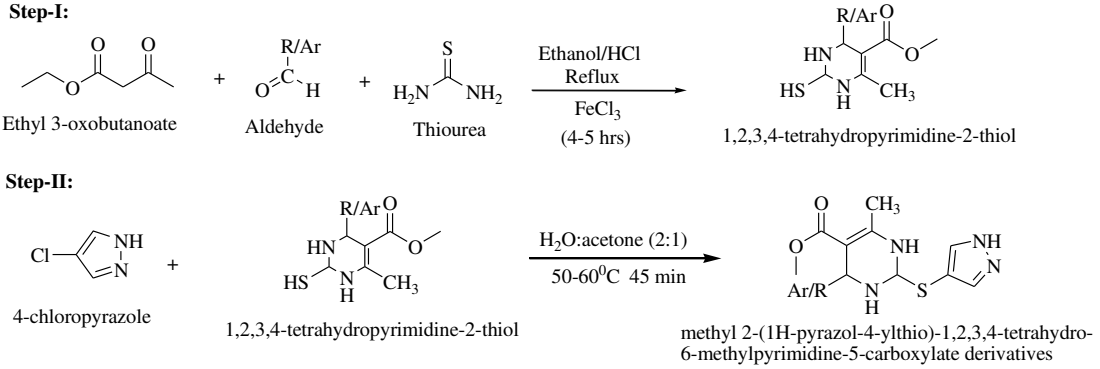

Figure 2. The proposed reaction scheme for the synthesis of methyl 2-(1H-pyrazol-4-ylthio)-1,2,3,4-tetrahydro-6-methylpyrimidine-5-carboxylate derivatives

Methyl 2-(1H-pyrazol-4-ylthio)-1,2,3,4-tetrahydro-6-methyl-4-p-tolylpyrimidine-5-carboxylate **(A7)**

Molecular formula: $C_{17}H_{20}N_4O_2S$, molecular weight: 344.3 gm/mol, appearance: pale yellow solid, melting point: 213-215 ^{0}C, Rf value: 0.64, yield: 73%, solubility: ethanol, methanol, dichloromethane (DCM), chloroform, and benzene. Elemental analysis (*calc.*): C, 42.42; H, 5.00; Cl, 9.63; Fe, 3.79; N, 15.22; O, 13.04; S, 10.89. ^{1}H NMR ($CHCl_3$-d_6 400 MHz) δ ppm: 1.829 (s, methyl protons of pyrimidine), 2.135 (s, N-H of pyrimidine), 2.461 (s, methyl protons of phenyl ring), 3.671 (s, methoxy protons of acetate), 4.621, 4.701 (d, methylene protons of pyrimidine), 6.908 (s, phenyl protons), 7.834 (s, methylene protons of diazole). ^{13}C NMR ($CHCl_3$-d_6 400 MHz) δ ppm: 15.980, 25.120, 52.901, 59.872, 76.902, 105.939, 106.001, 127.102, 128.582, 133.901, 136.291, 137.002, 154.091, 168.502. MS: m/z 345.34, 346.72 (m+1), 348.89 (m+2).

methyl 2-(1H-pyrazol-4-ylthio)-1,2,3,4-tetrahydro-6-methyl-4-(naphthalen-1-yl)pyrimidine-5-carboxylate **(A16)**

Molecular formula: $C_{20}H_{20}N_4O_2S$, molecular weight: 330.46 gm/mol, appearance: 221-223 ^{0}C, Rf values: 0.82, yield: 68%, solubility: ethanol, methanol, DCM, chloroform. Elemental analysis (*calc.*): C, 63.14; H, 5.30; N, 14.73; O, 8.41; S, 8.43. ^{1}H NMR ($CHCl_3$-d_6 400 MHz) δ ppm: 1.709 (s, methyl protons of pyrimidine), 2.205 (s, N-H of pyrimidine), 3.771 (s, methoxy protons of acetate), 4.671, 4.789 (d, methylene protons of pyrimidine), 6.908 (s, phenyl protons), 7.834 (s, methylene protons of diazole). 7.002, 7.128, 7.329, 7.571, 7.689, 7.790, 7.820, 7.981 (m, aromatic protons). ^{13}C NMR ($CHCl_3$-d_6 400 MHz) δ ppm: 14.003, 52.762, 56.990, 78.201, 104.891, 106.003, 124.201, 125.549, 126.889, 127.002, 128.652, 129.201, 132.781, 133.009, 134.310, 154.009, 168.980. MS: m/z 380.92, 381.89 (m+1), 382.91 (m+2).

methyl 2-(1H-pyrazol-4-ylthio)-4-(4-(trifluoromethyl)phenyl)-1,2,3,4-tetrahydro-6-methylpyrimidine-5-carboxylate **(A20)**

Molecular formula: $C_{17}H_{17}F_3N_4O_2S$, molecular weight: 398.4 gm/mol, melting point: 239-241 ^{0}C, Rf value: 0.73, yield: 81%, solubility: ethanol, methanol, DCM, chloroform, benzene. Elemental analysis (*calc.*): C, 51.25; H, 4.30; F, 14.31; N, 14.06; O, 8.03; S, 8.05. ^{1}H NMR ($CHCl_3$-d_6 400 MHz) δ ppm: 1.698 (s, methyl protons of pyrimidine), 2.009 (s, N-H of pyrimidine), 3.799 (s, methoxy protons of acetate), 4.721, 4.798 (d, methylene protons of pyrimidine), 6.991 (s, phenyl protons), 7.392 (s, phenyl protons), 7.781 (s, methylene protons of diazole). ^{13}C NMR ($CHCl_3$-d_6 400 MHz) δ ppm: 16.029, 52.710, 58.892, 78.680, 104.630, 106.009, 122.128, 123.459, 124.903, 125.671, 126.582, 127.709, 128.430, 134.829, 142.302, 154.002, 168.992. MS: m/z 399.01, 400.71 (m+1), 401.85 (m+2).

In vitro biological evaluation

Various concentrations of derivatives were prepared in DMSO to assess their antibacterial and antifungal activities against standard strains using broth dilution. Bacteria were maintained, and drugs were diluted in nutrient Mueller Hinton broth. The broth was inoculated with 10^8 colony-forming units (cfu) per milliliter of test strains (Institute of Microbial Technology, Chandigarh, India)

determined by turbidity. Stock solutions of synthesized derivate (2 mg/mL) were serially diluted for primary and secondary screening. The primary screen included 1000, 500, and 250 µg/mL of synthesized derivatives, then those with activity were further screened at 200, 100, 50, 25, 12.5, and 6.250 µg/mL. A control without antibiotic was sub-cultured (before inoculation) by spreading one loopful evenly over a quarter of a plate of medium suitable for growing test organisms and incubated at 37 ^{0}C overnight. The lowest concentrations of derivatives that inhibited bacterial or fungal growth were taken as minimal inhibitory concentrations (MICs). These were compared with the amount of control growth before incubation (original inoculum) to determine MIC accuracy. The standards for antibacterial activity were gentamycin, ampicillin, chloramphenicol, ciprofloxacin, and norfloxacin served, and those for antifungal activity were nystatin and griseofulvin. The antimalarial behavior was tested using plasmodium falciparum, with quinine and chloroquine as the standards. Both experiments took place at the Microcare laboratory and Tuberculosis Research Centre [TRC] in Surat, Gujarat.

Results

Pharmacokinetic characteristics are critical to drug development because they enable scientists to investigate the biological impacts of possible pharmacological candidates (Khan et al., 2022). This compound's oral bioavailability was evaluated using Lipinski's rule of five and Veber's rules (Table 2). To better understand the pharmacokinetics profiles and drug-likeness properties of the proposed compounds, the ADME characteristics of all of them were examined (Table 3). Fig. 3 depicts the physicochemical domain that is ideal for oral bioavailability. The oral acute toxicity have been predicted along with LD_{50} (mg/kg), toxicity class, hepatotoxicity, carcinogenicity, immunotoxicity, mutagenicity, and cytotoxicity (Table 4). Table 5 lists the ligand energies (kcal/mol), docking scores (kcal/mol), active amino acids, bond length (Å), and different interactions of derivatives with DHFR. Table 6 depicts the most potent compounds' 2D and 3D docking orientations. The results of antimicrobial and antifungal activities of the synthesized derivatives are tabulated in Table 7 which shows the MICs and MFCs respectively.

Table 2
Lipinski rule of 5 and Veber's rule calculated for methyl 2-(1*H*-pyrazol-4-ylthio)-1,2,3,4-tetrahydro-6-methylpyrimidine-5-carboxylate derivatives

Compound Codes	Lipinski rule of five					Veber's rule	
	Log P	Mol. Wt.	HBA	HBD	Violations	Total polar surface area (Å^2)	No. of rotatable bonds
NL	0.70	443.45	7	6	2	187.50	10
A1	0.56	254.31	4	3	0	104.34	4
A2	1.75	330.40	4	3	0	104.34	5
A3	-0.25	376.41	6	6	0	154.00	6
A4	2.38	409.30	4	3	0	104.34	5
A5	2.06	348.40	5	3	0	104.34	5

A6	2.30	364.85	4	3	0	104.34	5
A7	2.11	344.43	4	3	0	104.34	5
A8	1.78	360.25	5	3	0	113.57	6
A9	1.37	346.40	5	4	0	124.57	5
A10	-0.15	376.41	6	4	0	154.00	6
A11	1.38	346.40	5	4	0	124.57	5
A12	0.76	378.40	7	6	1	165.75	5
A13	1.37	376.43	6	4	0	133.34	6
A14	1.75	360.43	5	3	0	113.57	6
A15	2.30	356.44	4	3	0	104.34	6
A16	2.61	380.46	4	3	0	104.34	5
A17	2.61	380.46	4	3	0	104.34	5
A18	1.44	408.50	6	3	0	146.86	6
A19	1.80	373.47	4	3	0	107.58	6
A20	1.80	373.47	4	3	0	107.58	6

Where: NL, native ligand; Mol. Wt., molecular weight; HBA, hydrogen bond acceptors; HBD, hydrogen bond donors

Table 3
The pharmacokinetics and drug-likeness properties of developed compounds

Compound codes	Pharmacokinetics									Drug-likeness			
	GI abs.	BBB pen.	P-gp sub.	CYP 1A2	CYP 2C19	CYP 2C9	CYP 2D6	CYP 3A4	Log K_p (skin permeation, cm/s)	Ghose	Egan	Muegge	Bioavailability Score
				inhibitors									
NL	L	N	Y	N	N	N	N	N	-8.81	Y	N	N	0.11
A1	H	N	N	N	N	N	N	N	-7.40	Y	Y	Y	0.55
A2	H	N	Y	N	N	N	N	N	-6.67	Y	Y	Y	0.55
A3	L	N	Y	N	N	N	N	N	-7.40	Y	N	N	0.55
A4	H	N	Y	N	Y	N	N	Y	-6.66	Y	Y	Y	0.55
A5	H	N	Y	N	N	N	N	N	-6.71	Y	Y	Y	0.55
A6	H	N	Y	N	Y	N	N	Y	-6.43	Y	Y	Y	0.55
A7	H	N	Y	N	N	N	N	Y	-6.49	Y	Y	Y	0.55
A8	H	N	Y	N	N	N	N	Y	-6.87	Y	Y	Y	0.55
A9	H	N	Y	N	N	N	N	N	-7.01	Y	Y	Y	0.55
A10	L	N	Y	N	N	N	N	N	-7.40	Y	N	N	0.55
A11	H	N	Y	N	N	N	N	N	-7.01	Y	Y	Y	0.55
A12	L	N	Y	N	N	N	N	N	-7.71	Y	N	N	0.55
A13	H	N	Y	N	N	N	N	N	-7.22	Y	N	Y	0.55
A14	H	N	Y	N	N	N	N	Y	-6.87	Y	Y	Y	0.55
A15	H	N	Y	Y	N	Y	N	N	-6.37	Y	Y	Y	0.55
A16	H	N	Y	N	Y	Y	Y	Y	-6.09	Y	Y	Y	0.55
A17	H	N	Y	N	Y	Y	Y	Y	-6.09	Y	Y	Y	0.55
A18	L	N	Y	N	N	N	N	N	-7.68	Y	N	Y	0.55
A19	H	N	Y	N	N	N	N	Y	-6.84	Y	Y	Y	0.55
A20	H	N	Y	N	N	N	N	Y	-6.68	Y	Y	Y	0.55

Where: NL, Native ligand; GI abs., gastrointestinal absorption; BBB pen, blood brain barrier penetration; P-gp sub., p-glycoprotein substrate

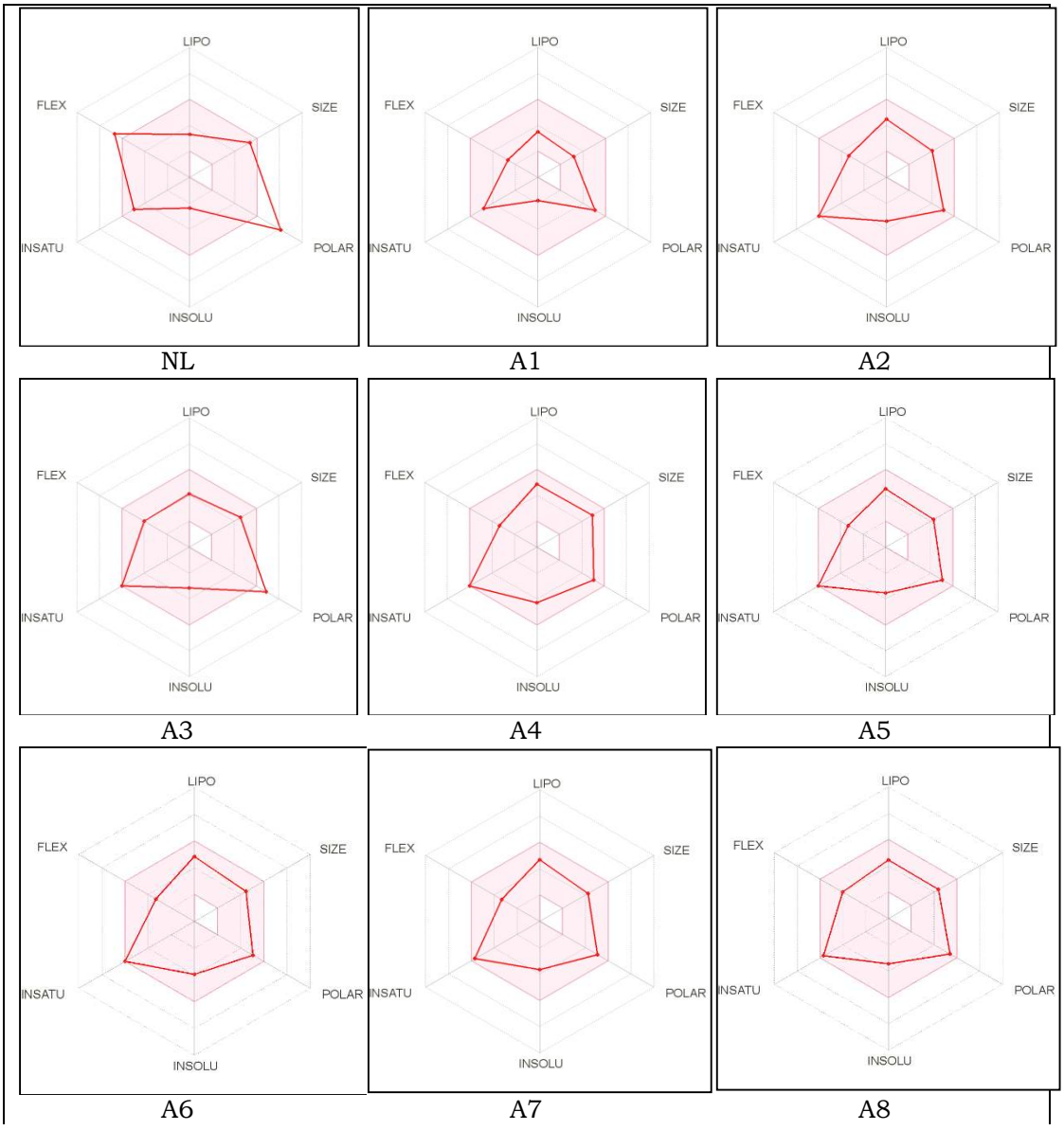
LIPO
SIZE
POLAR
INSOLU
INSATU
FLEX
NL
A1
A2
A3
A4
A5
A6
A7
A8

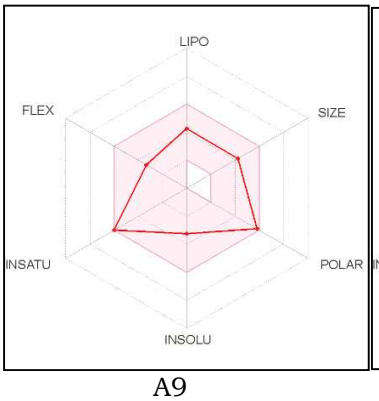

A9

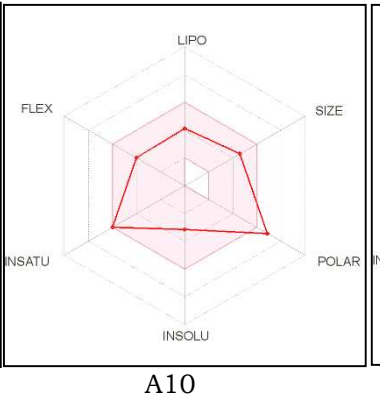

A10

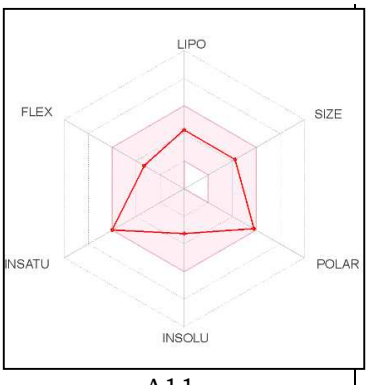

A11

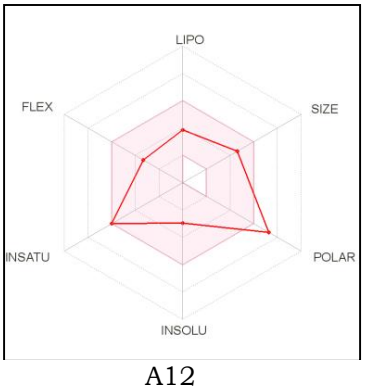

A12

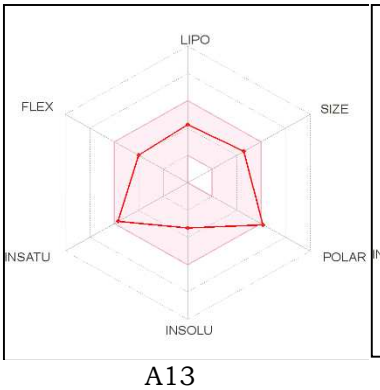

A13

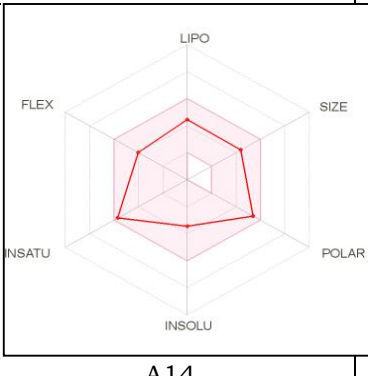

A14

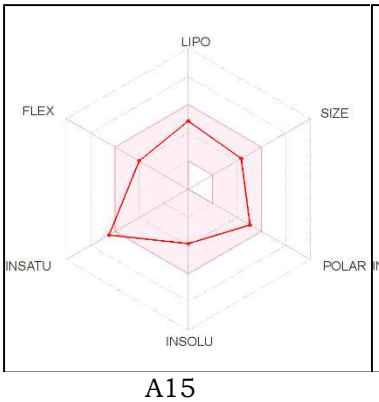

A15

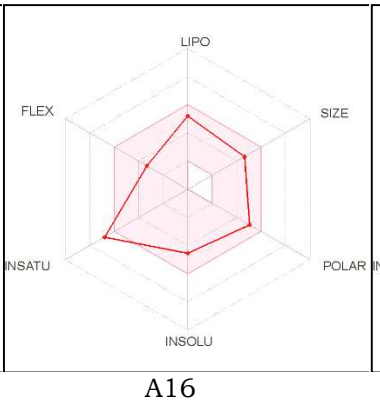

A16

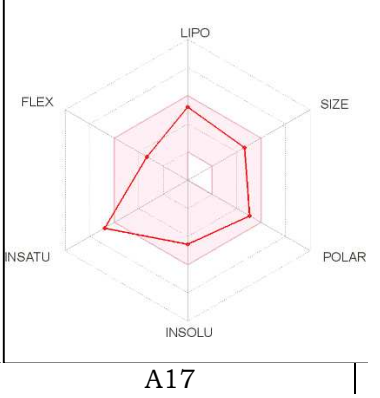

A17

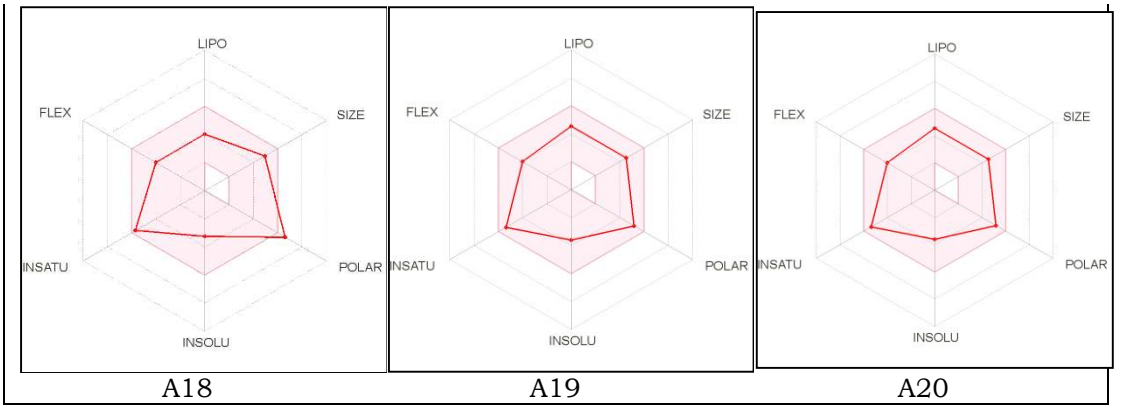

Figure 3. The coloured zone is the acceptable physicochemical area for oral bioavailability, according to the physicochemical radar of the molecules. Where, LIPO (Lipophility): -0.7<XLOGP3<+5.0, SIZE: 150g/mol<MV<500g/mol, POLAR (Polarity): 20Å^2<TPSA<130Å^2, INSOLU (Insolubility): 0<LogS (ESOL)<6, INSATU (Instauration): 0.25<Fraction Csp3<1, FLEX (Flexibility): 0<Num. of rotatable bonds<9

Table 4
The predicted acute toxicities of the designed methyl 2-(1*H*-pyrazol-4-ylthio)-1,2,3,4-tetrahydro-6-methylpyrimidine-5-carboxylate derivatives

Compound codes	Parameters							
	LD_{50} (mg/kg)	Toxicity class	Prediction accuracy (%)	Hepatotoxicity (Probability)	Carcinogenicity (Probability)	Immunotoxicity (Probability)	Mutagenicity (Probability)	Cytotoxicity (Probability)
NL	135	3	67.38	I (0.87)	I (0.51)	I (0.99)	I (075)	I (0.63)
A1	1353	4	54.26	A (0.51)	A (0.53)	I (0.78)	I (0.60)	I (0.65)
A2	1644	4	23	A (0.67)	A (0.52)	I (0.95)	I (0.63)	I (0.69)
A3	1000	4	54.26	A (0.67)	A (0.52)	I (0.95)	I (0.63)	I (0.69)
A4	1644	4	23	A (0.69)	I (0.53)	I (0.70)	I (0.69)	I (0.64)
A5	2000	4	12	A (0.70)	I (0.54)	I (0.66)	I (0.68)	I (0.69)
A6	630	4	23	A (0.67)	I (0.54)	I (0.78)	I (0.68)	I (0.69)
A7	1644	4	23	A (0.65)	A (0.50)	I (0.96)	I (0.63)	I (0.70)
A8	785	4	23	A (0.65)	A (0.51)	I (0.68)	I (0.62)	I (0.73)
A9	1644	4	23	A (0.68)	A (0.56)	I (0.87)	I (0.62)	I (0.72)
A10	1000	4	54.26	A (0.68)	A (0.56)	I (0.87)	I (0.62)	I (0.72)
A11	1644	4	23	A(0.68)	A (0.56)	I (0.55)	I (0.62)	I (0.72)
A12	150	3	54.26	A (0.66)	A (0.54)	A (0.68)	I (0.61)	I (0.75)
A13	3000	5	54.26	A (0.65)	A (0.53)	A (0.88)	I (0.60)	I (0.77)
A14	3000	5	54.26	A (0.65)	A (0.51)	A (0.58)	I (0.61)	I (0.76)
A15	880	4	23	A (0.66)	A (0.52)	I (0.79)	I (0.65)	I (0.69)
A16	880	4	23	A (0.66)	A (0.52)	I (0.79)	I (0.65)	I (0.69)
A17	50	2	54.26	A (0.66)	A (0.54)	A (0.68)	I (0.61)	I (0.75)
A18	1644	4	23	A (0.50)	I (0.52)	I (0.71)	I (0.70)	I (0.65)
A19	1700	4	54.26	A (0.56)	A (0.50)	I (0.60)	I (0.58)	I (0.67)
A20	1644	4	23	A (0.68)	I (0.51)	I (0.80)	I (0.65)	I (0.68)

Where: NL, Native ligand; I, Inactive; A, Active

Table 5
The ligand energies (kcal/mol), docking scores (kcal/mol), active amino acids, bond length (Å), and different interactions of derivatives with DHFR

Interactive amino acid residues	Bond length (Å)	Bond type	Bond category	Ligand energy (kcal/mol)	Docking score (kcal/mol)
Native ligand					
ASP27	1.88237	Hydrogen bond	Conventional hydrogen bond	209.71	-8.5
ASP27	2.19462				
ALA6	3.00495				
ILE5	1.91594				
ARG57	1.96549				
ARG57	2.17225				
ILE94	3.19208		Carbon hydrogen bond		
ILE50	3.71343	Hydrophobic	Pi-Sigma		
PHE31	5.0747		Pi-Pi T-shaped		
PHE31	4.82737				
ILE94	4.98884		Alkyl		
ILE5	5.06209		Pi-Alkyl		
ALA7	4.05078				
A1					
ILE5	3.0749	Hydrogen bond	Conventional hydrogen bond	370.2	-6.2
SER49	2.16739				
GLY15	3.36144		Carbon hydrogen bond		
A2					
TRP22	2.27723	Hydrogen bond	Conventional hydrogen bond	482.71	-7.7
MET20	2.49262				
TRP22	2.93754				
TRP22	3.1677		Pi-donor hydrogen bond		
PHE31	4.77582	Hydrophobic	Pi-Pi T-shaped		
ALA7	4.21529		Pi-alkyl		
A3					
GLU17	5.51927	Electrostatic	Attractive charge	497.76	-8.4
ALA6	2.67178	Hydrogen bond	Conventional hydrogen bond		
MET20	2.5286				
TRP22	2.76005				
TRP22	2.47537				
TRP30	3.35802		Carbon hydrogen bond		
ASP27	3.89344	Electrostatic	Pi-anion		
TRP22	3.0994	Hydrogen bond	Pi-donor hydrogen bond		
ALA7	4.11348	Hydrophobic	Pi-alkyl		

1030

A4					
TRP22	2.29725	Hydrogen bond	Conventional hydrogen bond	481.01	-7.4
MET20	2.61225				
TRP22	2.837				
GLU17	3.7728		Carbon hydrogen bond		
ASP27	3.90453	Electrostatic	Pi-anion		
TRP22	3.15968	Hydrogen bond	Pi-donor hydrogen bond		
PHE31	4.79282	Hydrophobic	Pi-Pi T-shaped		
ILE5	4.33985		Alkyl		
ALA7	4.22771		Pi-alkyl		
TRP30	4.75628				
PHE31	5.23494				
A5					
MET20	2.49522	Hydrogen bond	Conventional hydrogen bond	482.22	-8
TRP22	2.33951				
TRP22	3.17129		Pi-donor hydrogen bond		
PHE31	4.76537	Hydrophobic	Pi-Pi T-shaped		
ALA7	4.22612		Pi-alkyl		
A6					
TRP22	2.29725	Hydrogen bond	Conventional hydrogen bond	481.4	-8.1
MET20	2.61225				
TRP22	2.837				
GLU17	3.7728		Carbon hydrogen bond		
ASP27	3.90453	Electrostatic	Pi-Anion		
TRP22	3.15968	Hydrogen bond	Pi-donor hydrogen bond		
PHE31	4.79282	Hydrophobic	Pi-Pi T-shaped		
ILE5	4.33985		Alkyl		
ALA7	4.22771		Pi-alkyl		
TRP30	4.75628				
PHE31	5.23494				
A7					
TRP22	2.35415	Hydrogen bond	Conventional hydrogen bond	481.73	-8.3
MET20	2.55305				
TRP22	2.83361				
GLU17	3.68313		Carbon hydrogen bond		
ASP27	3.98723	Electrostatic	Pi-anion		
TRP22	3.11616	Hydrogen bond	Pi-donor hydrogen bond		
ILE5	4.40098	Hydrophobic	Alkyl		
ALA7	4.23804		Pi-alkyl		
TRP30	5.08623				

PHE31	5.10624				
A8					
GLU17	4.95931	Electrostatic	Attractive charge	495	-7.8
MET20	2.72705	Hydrogen bond	Conventional hydrogen bond		
TRP22	2.67773				
MET20	2.6585				
TRP22	2.48262				
ASP27	3.31806		Carbon hydrogen bond		
PHE31	4.92417	Hydrophobic	Pi-Pi T-shaped		
ILE5	4.3573		Alkyl		
ALA7	4.30898		Pi-alkyl		
TRP30	4.83273				
PHE31	5.35704				
A9					
TRP22	2.36338	Hydrogen bond	Conventional hydrogen bond	481.76	-7.8
MET20	2.60446				
TRP22	2.79657				
ASP27	2.19355				
GLU17	3.72159		Carbon hydrogen bond		
ASP27	3.74291	Electrostatic	Pi-anion		
TRP22	3.11835	Hydrogen bond	Pi-donor hydrogen bond		
ALA7	4.26215	Hydrophobic	Pi-alkyl		
A11					
ASN23	2.2316	Hydrogen bond	Conventional hydrogen bond	496.05	-7.7
ALA7	2.32527				
ILE94	3.56597		Carbon hydrogen bond		
ASP27	4.39963	Electrostatic	Pi-anion		
ALA7	4.35161	Hydrophobic	Pi-alkyl		
A13					
ASN23	2.38748	Hydrogen Bond	Conventional hydrogen bond	539.67	-7.9
ALA7	2.37703				
ILE94	3.62461		Carbon hydrogen bond		
ASP27	4.45997	Electrostatic	Pi-anion		
ALA7	4.51712	Hydrophobic	Pi-alkyl		
A14					
MET20	2.99811	Hydrogen bond	Conventional hydrogen bond	953.03	-7.9
SER49	3.76564		Carbon hydrogen bond		
ASP27	3.62766				
MET20	3.78648	Hydrophobic	Pi-sigma		
PHE31	5.63444		Pi-Pi T-shaped		
ALA6	5.27008		Pi-alkyl		

ILE14	5.13588				
A15					
GLY15	2.67824	Hydrogen bond	Conventional hydrogen bond	409.54	-7.6
ILE94	3.71793		Carbon hydrogen bond		
PHE31	3.24001		Pi-donor hydrogen bond		
LEU28	5.12782	Hydrophobic	Pi-alkyl		
LYS32	4.84966				
LEU54	5.36449				
A16					
LEU28	2.14171	Hydrogen bond	Conventional hydrogen bond	525.12	-8.4
SER49	3.45221		Carbon hydrogen bond		
GLU17	3.58115				
ILE94	5.04659	Hydrophobic	Pi-alkyl		
ALA7	4.80042				
A19					
TYR100	2.09124	Hydrogen bond	Conventional hydrogen bond	778.91	-7.4
ASN23	3.54082		Carbon hydrogen bond		
TRP22	3.3755				
ASN23	3.69258				
THR46	3.40368				
LEU28	3.6598	Hydrophobic	Pi-sigma		
PHE31	5.91152		Pi-Pi T-shaped		
LEU28	4.35494		Alkyl		
ILE50	4.97052		Pi-alkyl		
MET20	5.3679				
A20					
ALA6	2.94081	Hydrogen bond;halogen	Conventional hydrogen bond;halogen (Fluorine)	495.95	-8.5
THR113	2.72271				
ALA7	3.54666	Hydrogen bond	Carbon hydrogen bond		
TRP30	3.42477				
ILE5	3.68896	Halogen	Halogen (Fluorine)		
ALA6	3.22298				
ALA6	3.07251				
ASP27	3.59766				
ASP27	2.91049				
ASP27	2.92109				
ASP27	3.05047				
ILE5	4.55123	Hydrophobic	Alkyl		
ALA7	4.19901				
ILE5	5.35857		Pi-Alkyl		

ALA7	4.63904				
TRP30	5.40442				
PHE31	5.47595				

Table 6
The 2D- and 3D binding orientations of native ligand and molecules selected for the synthesis from virtual screening

2D-binding orientations	3D-binding orientations
Native ligand	
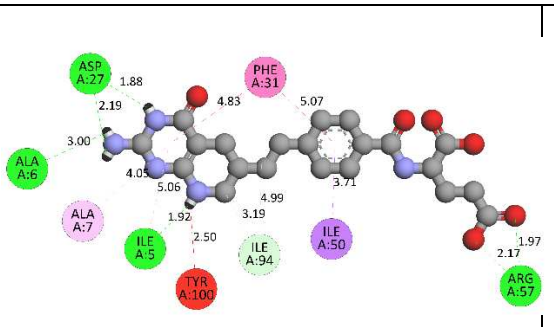	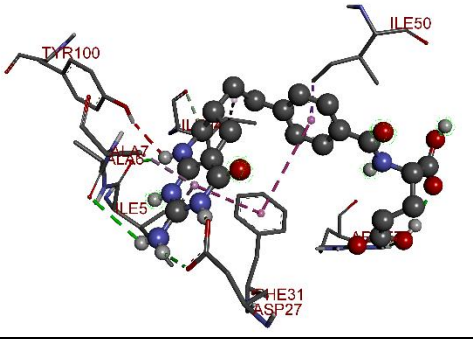
A7	
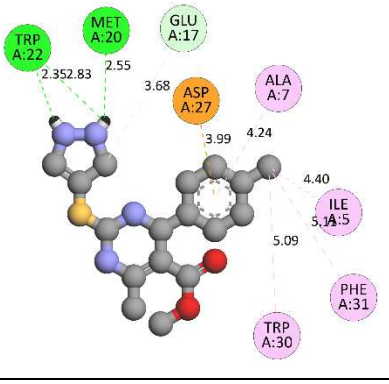	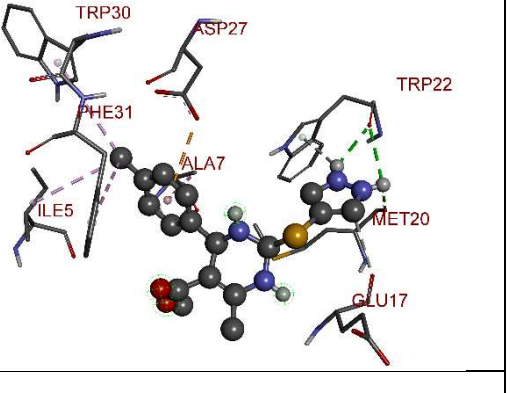
A16	
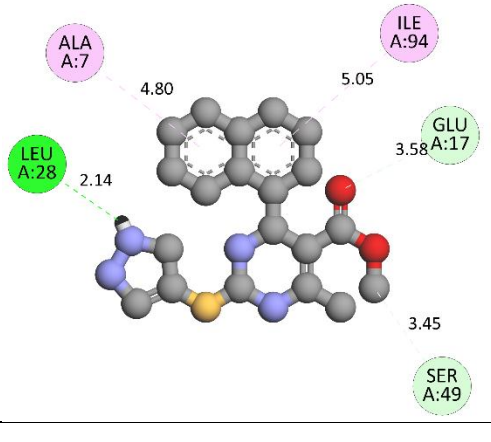	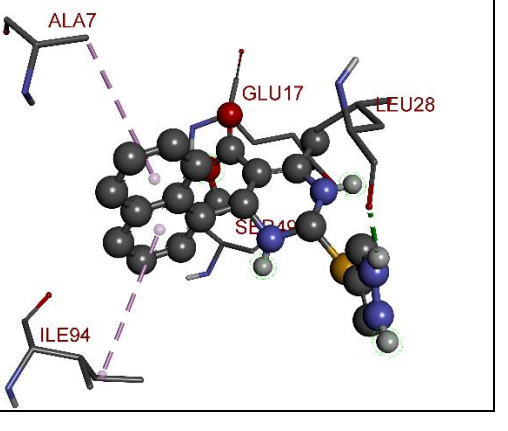

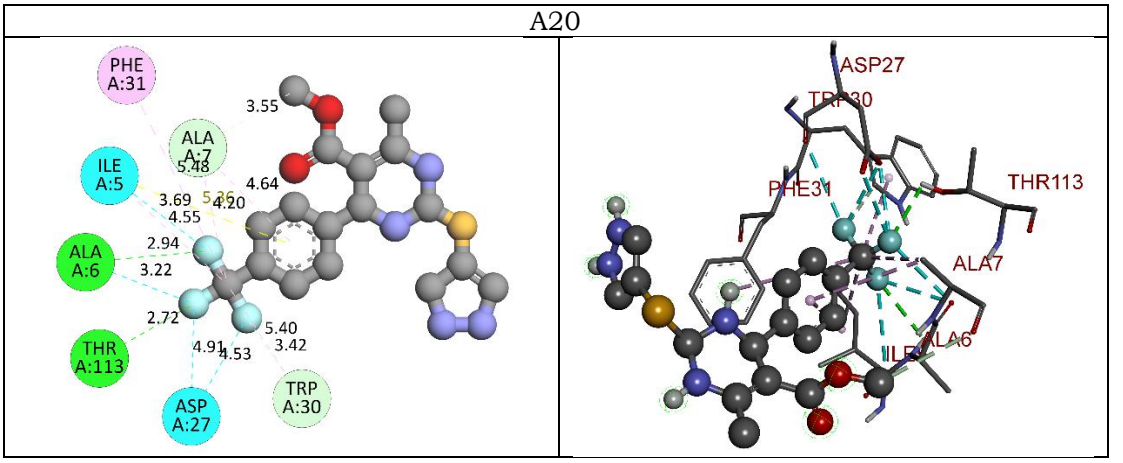

Table 7
The antimicrobial and antifungal activities of the synthesized derivatives

Compound code	Antimicrobial activity [*MIC* (µg/mL)]				Antifungal activity [*MFC* (µg/mL)]		
	E.C.	*P.A.*	*S.A.*	*S.P.*	*C.A.*	*A.N.*	*A.C.*
A7	25	25	25	50	100	100	100
A16	50	50	50	50	200	200	200
A20	25	25	25	25	100	200	100
Gentamycin	0.05	1	0.25	0.5	NA	NA	NA
Ampicillin	100	NA	250	100	NA	NA	NA
Chloramphenicol	50	50	50	50	NA	NA	NA
Ciprofloxacin	25	25	50	50	NA	NA	NA
Norfloxacine	10	10	10	10	NA	NA	NA
Nystatin	NA	NA	NA	NA	100	100	100
Greseofulvin	NA	NA	NA	NA	500	100	100

Where: E.C., Escherichia coli; P.A., Pseudomonas aeruginosa; S.A., Staphylococcus aureus; S.P., Staphylococcus pyogenes; C.A., Candida albicans; A.N., Aspergillus niger; A.C., Aspergillus clavatus; MIC, Minimum inhibitory concentration; MFCs, minimum fungicidal concentration.

Discussion

In present study we have designed and developed some methyl 2-(1H-pyrazol-4-ylthio)-1,2,3,4-tetrahydro-6-methylpyrimidine-5-carboxylate derivatives as potential DHFR inhibitors. In accordance with Lipinski's and Veber's rule (Table 2), few molecules has violated both the rules. The log P values of all the molecules found between -0.15 to 2.61 which indicate optimum lipophilicity. Lipophilicity is a significant feature of the molecule that affects how it works in the body(S. Khan et al., 2021). It is determined by the compound's Log P value, which measures the drug's permeability in the body to reach the target tissue(Krzywinski and Altman, 2013; Lipinski et al., 2012). The molecular weight of all the molecules was below 500 Da which indicates active better transport of the molecules through biological

membrane. Fortunately, the Lipinski rule of 5 had not been compromised by the compounds, excluding native ligand and compound A12, which displayed 2 and 1 violations of Lipinski rule respectively(Khan et al., 2022; Shntaif et al., 2021). The total polar surface area (TPSA) and the number of rotatable bonds has been found to better discriminate between compounds that are orally active or not. According to Veber's rule, TPSA should be ≤ 140 and number of rotatable bonds should be ≤ 10. It was observed that native ligand violated the Veber's rule, as it has TPSA 187.50Å2 and number of rotatable bonds 10 which indicate its poor oral bioavailability. Molecules A3, A10, A12, and A18 has showed more TPSA than acceptable value therefore these compounds were indicated poor oral bioavailability.

In order to further optimize the compounds, pharmacokinetics and drug-likeness properties were calculated for each one. All the compounds including native ligand showed no penetration to the blood-brain barrier (BBB). The log Kp (skin penetration, cm/s) and bioavailability values of all the compounds were within acceptable limits. Few molecules and native ligand do not meet all, two, or one of the Ghose, Egan, and Muegge requirements (Table 3). Molecules A3, A10, A12, A18, and native ligand exhibited low gastrointestinal (GI) absorption. In acute toxicity predictions, one molecule i.e. A17 falls in toxicity class-II [fatal if swallowed (5<LD50≤50)] whereas, native ligand and A12 fall in toxicity class-III i.e. toxic if swallowed (50<LD50≤300). Molecules A1-A11, A15, A16, and A18-A20 displayed toxicity class-IV which means harmful if swallowed (300<LD50≤2000). Molecules A13 and A14 showed toxicity class-V which indicate may be harmful if swallowed (2000<LD50≤5000)(Banerjee et al., 2018). From this virtual screening, it was concluded that compounds A3, A10, A12, A17, and A18 do not possess drug-like properties and hence were not subjected to molecular docking studies.

The binding affinities of the derivatives have been compared with the binding mode of native ligand present in the crystal structure of DHFR (PDB ID: 5CCC). Native ligand exhibited -8.5 kcal/mol binding affinity with DHFR and formed 6 conventional hydrogen bonds with Asp27, Ala6, Ile5, Arg57, and one carbon-hydrogen bond with Ile94. It has developed many hydrophobic interactions such as Pi-sigma, Pi-Pi T-shaped, alkyl, and Pi-alkyl bonds with Ile50, Phe31, Ile94, Ile5, and Ala7. Compound A7 exhibited -8.3 kcal/mol binding affinity and formed three conventional hydrogen bonds with Trp22 and Met20 whereas formed only one carbon-hydrogen bond with Glu17. It has developed one Pi-donor hydrogen bond with Trp22 and one electrostatic (Pi-anion) bond with Asp27. It displayed many hydrophobic interactions (alkyl and Pi-alkyl) with Ile5, Ala7, Trp30, and Phe31. Compound A16 displayed -8.4 kcal/mol docking score and formed only one conventional hydrogen bond Leu28 and two carbon-hydrogen bond with Ser49 and Glu17. It has developed Pi-allkyl interactions with Ile94 and Ala7. Compound A20 showed -8.5 kcal/mol binding affinity and developed two conventional hydrogen bonds with Ala6 and Thr113. It also formed two carbon-hydrogen bonds with Ala7 and Trp30. Most importantly it has developed halogen (fluorine) bonds with Ile5, Ala6, and Asp27. Compound A20 developed few hydrophobic (alkyl and Pi-alkyl) bonds with Ile5, Ala7, Trp30, and Phe31.

Millions of humans are now affected by bacterial diseases triggered by pathogenic bacteria which are responsible for elevated child mortality rates in developed countries [9]. Not all bacteria are pathogenic. For example, there are thousands of bacterial organisms in the human digestive tract, some of which are harmless and even useful. Furthermore, various mechanisms of action on the target site can aid in the discovery of potential drugs while developing antibacterial agents [10]. However, since bacteria have developed antibiotic tolerance, finding a new antibacterial agent became difficult. Gram-positive bacteria, such as methicillin-resistant S. aureus, S. epidermis, vancomycin-resistant E. calcium, and penicillin-resistant S. pneumoniae, induce the majority of bacterial infections. Fungal infections have become more frequent, and the majority of them are minor [11]. There are various varieties of fungi that cause infections today [12]. Species like candida and aspergillus are only a few examples [13]. In present investigation, all the synthesized compounds were subjected for in vitro antibacterial and antifungal activity using different strains as given in Table 7.

All the synthesized compounds were sensitive to both gram +ve (Staphylococcus aureus, Staphylococcus pyogenes) and gram –ve (Escherichia coli, Pseudomonas aeruginosa) bacterial strains. All the compounds demonstrated more potent activity than Ampicillin against both gram-positive and gram-negative bacteria. Most of the compounds were more or equipotent than Chloramphenicol and Ciprofloxacin. Compound A7 was sensitive at 25 μg/mL against Escherichia coli, Pseudomonas aeruginosa, and Staphylococcus aureus whereas compound A20 was sensitive to all gram +ve and –ve bacteria at same concentration. Compound A16 was sensitive at 50 μg/mL against all the bacteria. In antifungal activity, compound A7 exhibited MFCs of 100 μg/mL against Candida albicans, Aspergillus niger, and Aspergillus clavatus which is same as Nystatin. Compound A16 and A20 were also sensitive to all the antifungal strains at 100 or 200 μg/mL concentration. Compound A20 is more potent than Greseofulvin against Candida albicans. It can be concluded that substitution at para position with bulky group can greatly increase the activity of the designed compounds.

Conclusion

Dihydrofolate reductase (DHFR) is an important enzyme required to maintain bacterial growth, and hence inhibitors of DHFR have been proven as effective agents for treating bacterial infections. In present study we have designed and developed some methyl 2-(1H-pyrazol-4-ylthio)-1,2,3,4-tetrahydro-6-methylpyrimidine-5-carboxylate derivatives as potential DHFR inhibitors. The designed derivatives were screened through Lipinski rule, Veber's rule, ADMET analysis, drug-likeness properties, and molecular docking. The selected derivatives were synthesized and subjected for in vitro biological evaluation. We concluded that compounds A7, A16, and A20 are most potent and can developed further to get more promising molecules for the treatment of bacterial infection.

References

Ahmed Elkanzi, N.A., 2020. Synthesis and Biological Activities of Some Pyrimidine Derivatives: A Review. Orient. J. Chem. 36, 1001–1015. https://doi.org/10.13005/ojc/360602

Anwar, K., Hussein, D., Salih, J., 2020. Antimicrobial susceptibility testing and phenotypic detection of MRSA isolated from diabetic foot infection. Int. J. Gen. Med. 13, 1349–1357. https://doi.org/10.2147/IJGM.S278574

Banerjee, P., Eckert, A.O., Schrey, A.K., Preissner, R., 2018. ProTox-II: A webserver for the prediction of toxicity of chemicals. Nucleic Acids Res. 46, W257–W263. https://doi.org/10.1093/nar/gky318

Bhat, A.R., Dongre, R.S., Naikoo, G.A., Hassan, I.U., Ara, T., 2017. Proficient synthesis of bioactive annulated pyrimidine derivatives: A review. J. Taibah Univ. Sci. 11, 1047–1069. https://doi.org/10.1016/j.jtusci.2017.05.005

Chaudhari, R.N., Khan, S.L., Chaudhary, R.S., Jain, S.P., Siddiqui, F.A., 2020. B-Sitosterol: Isolation from Muntingia Calabura Linn Bark Extract, Structural Elucidation And Molecular Docking Studies As Potential Inhibitor of SARS-CoV-2 Mpro (COVID-19). Asian J. Pharm. Clin. Res. 13, 204–209. https://doi.org/10.22159/ajpcr.2020.v13i5.37909

Daina, A., Michielin, O., Zoete, V., 2017. SwissADME: A free web tool to evaluate pharmacokinetics, drug-likeness and medicinal chemistry friendliness of small molecules. Sci. Rep. 7. https://doi.org/10.1038/srep42717

Dallakyan, S., Olson, A.J., 2015. Small-molecule library screening by docking with PyRx. Methods Mol. Biol. 1263, 243–250. https://doi.org/10.1007/978-1-4939-2269-7_19

Durga devi, D., Manivarman, S., Subashchandrabose, S., 2017. Synthesis, molecular characterization of pyrimidine derivative: A combined experimental and theoretical investigation. Karbala Int. J. Mod. Sci. 3, 18–28. https://doi.org/10.1016/j.kijoms.2017.01.001

He, J., Qiao, W., An, Q., Yang, T., Luo, Y., 2020. Dihydrofolate reductase inhibitors for use as antimicrobial agents. Eur. J. Med. Chem. 195. https://doi.org/10.1016/j.ejmech.2020.112268

Indora, N., Kaushik, D., 2015. Design , development and evaluation of ethosomal gel of fluconazole for topical fungal infection. Int. J. Eng. Sci. Invent. Res. Dev. I, 280–306.

Jouhar, L., Jaafar, R.F., Nasreddine, R., Itani, O., Haddad, F., Rizk, N., Hoballah, J.J., 2020. Microbiological profile and antimicrobial resistance among diabetic foot infections in Lebanon. Int. Wound J. 17, 1764–1773. https://doi.org/10.1111/iwj.13465

Khan, A., Unnisa, A., Sohel, M., Date, M., Panpaliya, N., Saboo, S.G., Siddiqui, F., Khan, S., 2022. Investigation of phytoconstituents of Enicostemma littorale as potential glucokinase activators through molecular docking for the treatment of type 2 diabetes mellitus. Silico Pharmacol. 10. https://doi.org/10.1007/s40203-021-00116-8

Khan, S., Kale, M., Siddiqui, F., Nema, N., 2021. Novel pyrimidine-benzimidazole hybrids with antibacterial and antifungal properties and potential inhibition of SARS-CoV-2 main protease and spike glycoprotein. Digit. Chinese Med. 4, 102–119. https://doi.org/10.1016/j.dcmed.2021.06.004

Khan, S.L., Siddiqui, F.A., Jain, S.P., Sonwane, G.M., 2020. Discovery of Potential Inhibitors of SARS-CoV-2 (COVID-19) Main Protease (Mpro) from Nigella Sativa (Black Seed) by Molecular Docking Study. Coronaviruses 2, 384–402. https://doi.org/10.2174/2666796701999200921094103

Khan, S.L., Siddiqui, F.A., Shaikh, M.S., Nema, N. V., Shaikh, A.A., 2021. Discovery of potential inhibitors of the receptor-binding domain (RBD) of pandemic disease-causing SARS-CoV-2 Spike Glycoprotein from Triphala through molecular docking. Curr. Chinese Chem. 01. https://doi.org/10.2174/2666001601666210322121802

Khan, Sharuk L., Sonwane, G.M., Siddiqui, F.A., Jain, S.P., Kale, M.A., Borkar, V.S., 2020. Discovery of Naturally Occurring Flavonoids as Human Cytochrome P450 (CYP3A4) Inhibitors with the Aid of Computational Chemistry. Indo Glob. J. Pharm. Sci. 10, 58–69. https://doi.org/10.35652/igjps.2020.10409

Kim, S., Chen, J., Cheng, T., Gindulyte, A., He, J., He, S., Li, Q., Shoemaker, B.A., Thiessen, P.A., Yu, B., Zaslavsky, L., Zhang, J., Bolton, E.E., 2021. PubChem in 2021: New data content and improved web interfaces. Nucleic Acids Res. 49, D1388–D1395. https://doi.org/10.1093/nar/gkaa971

Krzywinski, M., Altman, N., 2013. Points of significance: Significance, P values and t-tests. Nat. Methods 10, 1041–1042. https://doi.org/10.1038/nmeth.2698

Lipinski, C.A., Lombardo, F., Dominy, B.W., Feeney, P.J., 2012. Experimental and computational approaches to estimate solubility and permeability in drug discovery and development settings. Adv. Drug Deliv. Rev. https://doi.org/10.1016/j.addr.2012.09.019

Liu, Q., Meng, X., Li, Y., Zhao, C.N., Tang, G.Y., Li, H. Bin, 2017. Antibacterial and antifungal activities of spices. Int. J. Mol. Sci. 18. https://doi.org/10.3390/ijms18061283

Loi, V. Van, Huyen, N.T.T., Busche, T., Tung, Q.N., Gruhlke, M.C.H., Kalinowski, J., Bernhardt, J., Slusarenko, A.J., Antelmann, H., 2019. Staphylococcus aureus responds to allicin by global S-thioallylation – Role of the Brx/BSH/YpdA pathway and the disulfide reductase MerA to overcome allicin stress. Free Radic. Biol. Med. 139, 55–69. https://doi.org/10.1016/j.freeradbiomed.2019.05.018

Manohar, P., Loh, B., Athira, S., Nachimuthu, R., Hua, X., Welburn, S.C., Leptihn, S., 2020. Secondary Bacterial Infections During Pulmonary Viral Disease: Phage Therapeutics as Alternatives to Antibiotics? Front. Microbiol. 11. https://doi.org/10.3389/fmicb.2020.01434

Marchese, A., Barbieri, R., Sanches-Silva, A., Daglia, M., Nabavi, S.F., Jafari, N.J., Izadi, M., Ajami, M., Nabavi, S.M., 2016. Antifungal and antibacterial activities of allicin: A review. Trends Food Sci. Technol. 52, 49–56. https://doi.org/10.1016/j.tifs.2016.03.010

Mittersteiner, M., Farias, F.F.S., Bonacorso, H.G., Martins, M.A.P., Zanatta, N., 2021. Ultrasound-assisted synthesis of pyrimidines and their fused derivatives: A review. Ultrason. Sonochem. 79. https://doi.org/10.1016/j.ultsonch.2021.105683

Mohana Roopan, S., Sompalle, R., 2016. Synthetic chemistry of pyrimidines and fused pyrimidines: A review. Synth. Commun. 46, 645–672. https://doi.org/10.1080/00397911.2016.1165254

Murali, T.S., Kavitha, S., Spoorthi, J., Bhat, D. V., Prasad, A.S.B., Upton, Z., Ramachandra, L., Acharya, R. V., Satyamoorthy, K., 2014. Characteristics of microbial drug resistance and its correlates in chronic diabetic foot ulcer infections. J. Med. Microbiol. 63, 1377–1385. https://doi.org/10.1099/jmm.0.076034-0

Nerkar, A.U., 2021. Use of Pyrimidine and Its Derivative in Pharmaceuticals: A Review. J. Adv. Chem. Sci. 7, 729–732. https://doi.org/10.30799/jacs.239.21070203

Qin, H.L., Zhang, Z.W., Lekkala, R., Alsulami, H., Rakesh, K.P., 2020. Chalcone hybrids as privileged scaffolds in antimalarial drug discovery: A key review. Eur. J. Med. Chem. 193. https://doi.org/10.1016/j.ejmech.2020.112215

Rahman, M., Hasan, M.F., Das, R., Khan, A., 2009. The Determination of Antibacterial and Antifungal Activities of Polygonum hydropiper (L.) Root Extract. Adv. Biol. Res. (Rennes). 3, 53–56.

Rappé, A.K., Casewit, C.J., Colwell, K.S., Goddard, W.A., Skiff, W.M., 1992. UFF, a Full Periodic Table Force Field for Molecular Mechanics and Molecular Dynamics Simulations. J. Am. Chem. Soc. 114, 10024–10035. https://doi.org/10.1021/ja00051a040

Reta, A., Bitew Kifilie, A., Mengist, A., 2019. Bacterial Infections and Their Antibiotic Resistance Pattern in Ethiopia: A Systematic Review. Adv. Prev. Med. 2019, 1–10. https://doi.org/10.1155/2019/4380309

San Diego: Accelrys Software Inc., 2012. Discovery Studio Modeling Environment, Release 3.5. Accelrys Softw. Inc.

Sanchez, E., Doron, S., 2016. Bacterial Infections: Overview, in: International Encyclopedia of Public Health. pp. 196–205. https://doi.org/10.1016/B978-0-12-803678-5.00030-8

Sánchez-Sánchez, M., Cruz-Pulido, W.L., Bladinieres-Cámara, E., Alcalá-Durán, R., Rivera-Sánchez, G., Bocanegra-García, V., 2017. Bacterial Prevalence and Antibiotic Resistance in Clinical Isolates of Diabetic Foot Ulcers in the Northeast of Tamaulipas, Mexico. Int. J. Low. Extrem. Wounds 16, 129–134. https://doi.org/10.1177/1534734617705254

Shen, Z.L., Xu, X.P., Ji, S.J., 2010. Brønsted base-catalyzed one-pot three-component Biginelli-type reaction: An efficient synthesis of 4,5,6-triaryl-3,4-dihydropyrimidin-2(1H)-one and mechanistic study. J. Org. Chem. 75, 1162–1167. https://doi.org/10.1021/jo902394y

Shntaif, A.H., Khan, S., Tapadiya, G., Chettupalli, A., Saboo, S., Shaikh, M.S., Siddiqui, F., Amara, R.R., 2021. Rational drug design, synthesis, and biological evaluation of novel N-(2-arylaminophenyl)-2,3-diphenylquinoxaline-6-sulfonamides as potential antimalarial, antifungal, and antibacterial agents. Digit. Chinese Med. 4, 290–304. https://doi.org/10.1016/j.dcmed.2021.12.004

Siddiqui, F.A., Khan, S.L., Marathe, R.P., Nema, N. V., 2021. Design, Synthesis, and In Silico Studies of Novel N-(2-Aminophenyl)-2,3- Diphenylquinoxaline-6-Sulfonamide Derivatives Targeting Receptor- Binding Domain (RBD) of SARS-CoV-2 Spike Glycoprotein and their Evaluation as Antimicrobial and Antimalarial Agents. Lett. Drug Des. Discov. 18, 915–931. https://doi.org/10.2174/1570180818666210427095203

Songsungthong, W., Prasopporn, S., Bohan, L., Srimanote, P., Leartsakulpanich, U., Yongkiettrakul, S., 2021. A novel bicyclic 2,4-diaminopyrimidine inhibitor

of Streptococcus suis dihydrofolate reductase. PeerJ 9. https://doi.org/10.7717/peerj.10743

Verma, V., Joshi, C.P., Agarwal, A., Soni, S., Kataria, U., 2020. A Review on Pharmacological Aspects of Pyrimidine Derivatives. J. Drug Deliv. Ther. 10, 358–361. https://doi.org/10.22270/jddt.v10i5.4295

Wróbel, A., Arciszewska, K., Maliszewski, D., Drozdowska, D., 2020. Trimethoprim and other nonclassical antifolates an excellent template for searching modifications of dihydrofolate reductase enzyme inhibitors. J. Antibiot. (Tokyo). 73, 5–27. https://doi.org/10.1038/s41429-019-0240-6